Removal of bacteria *Legionella pneumophila*, *Escherichia coli*, and *Bacillus subtilis* by (super)cavitation

Andrej Šarc[1], Janez Kosel[1], David Stopar[2], Martina Oder[3], Matevž Dular[1*]

[1]University of Ljubljana, Faculty of Mechanical Engineering, Askerceva 6, 1000 Ljubljana, Slovenia

[2]University of Ljubljana, Biotechnical Faculty, Večna pot 111, 1000 Ljubljana, Slovenia

[3]University of Ljubljana, Faculty of Health Sciences, Zdravstvena pot 5, 1000 Ljubljana, Slovenia

Abstract

In sufficient concentrations, the pathogenic bacteria *L. pneumophila* can cause a respiratory illness that is known as the "Legionnaries" disease. Moreover, toxic Shiga strains of bacteria *E. coli* can cause life-threatening hemolytic-uremic syndrome. Because of the recent restrictions imposed on the usage of chlorine, outbreaks of these two bacterial species have become more common. In this study we have developed a novel rotation generator and its effectiveness against bacteria *Legionella pneumophila* and *Escherichia coli* was tested for various types of hydrodynamic cavitation (attached steady cavitation, developed unsteady cavitation and supercavitation). The results show that the supercavitation was the only effective form of cavitation. It enabled more than 3 logs reductions for both bacterial species and was also effective against a more persistent Gram positive bacteria, *B. subtilis*. The deactivation mechanism is at present unknown. It is proposed that when bacterial cells enter a supercavitation

cavity, an immediate pressure drop occurs and this results in bursting of the cellular membrane. The new rotation generator that induced supercavitation proved to be economically and microbiologically far more effective than the classical Venturi section (super)cavitation.

Key words: Cavitation, Supercavitation, Bacteria, *E. coli*, *L. pneumophila* and *B. subtilis*, rotational cavitation generator

1 Introduction

In developed countries, diseases caused by pathogenic bacteria are still a major cause of human death. Chlorination is the usual method applied, however it has several shortcomings, among them the formation of dangerous organochlorides and the need for careful control of chlorine dosing (Mezule et al., 2009). Therefore, there is a strong initiative to develop effective, safe, easy to perform and less labour-intensive methods. One of the more attractive methods is hydrodynamic cavitation (Dular et al., 2016).

Cavitation is a physical phenomenon involving appearance of vapour bubbles in an initially homogeneous liquid due to the decrease of local pressure at an approximately constant temperature (Franc and Michel, 2004). The application of acoustic cavitation for the inactivation of bacteria has been extensively studied (Hulsmans et al., 2010) and although this method proved to be efficient, it is energy demanding and cannot be adopted for large scale industrial volumes (Gogate and Pandit, 2004). On the other hand, hydrodynamic cavitation can be more easily scaled up for potential industrial applications. It is formed when inception, growth and collapse of vapour bubbles are the result of an increase in fluid velocity and a simultaneous decrease in

46 static pressure. Depending on the inlet fluid velocities, three forms of hydrodynamic cavitation
47 can develop: attached steady cavitation, developed unsteady cavitation and supercavitation. In
48 the case of attached steady cavitation, the vapour phase does not significantly affect the liquid
49 flow. This is no longer true for developed unsteady cavitation as the large volume of vapour
50 drastically changes the liquid flow (Franc, 2006). Developed unsteady cavitation is characterised
51 by cavitation clouds shedding, accompanied by the generation of various physical (pressure
52 pulses, shear forces, high temperatures) and chemical effects (OH^- production) that can be
53 employed for the removal of pathogenic microorganisms (Riesz and Kondo, 1992; von Eiff et
54 al., 2000). Supercavitation occurs at very low pressures and/or high velocities where a large and
55 stable vapour cavity develops (Stinebring et al., 2001). Within this single vapour cavity larger
56 disturbances in pressure and temperature are uncommon and consequently it could be expected
57 that supercavitation does not cause any substantial damage to bacterial cells (Dommerich et al.,
58 2012). Nonetheless, Šarc et al. (2016) observed that after 60 min of treatment in Venturi
59 constriction, supercavitation removed 98.6 % of bacteria *L. pneumophila*, while developed
60 unsteady cavitation removed only 28.0 % of the viable count. Although a reduction of 98.6 % by
61 supercavitaiton is promising (that is a 1.8 logs reduction of the initial concentration of 5.0
62 $Log_{10}CFUmL^{-1}$ to a final concentration of 3.2 $Log_{10}CFUmL^{-1}$), this reduction is still lower than 2
63 logs and is therefore inappropriate for the use in waste water treatments. Only stronger
64 treatments that can reduce the viable count to around 2.0 $Log_{10}CFUmL^{-1}$ can be successfully
65 used to prevent infections, such as cholera, typhoid fever and shigellosis (Exner et al., 2003;
66 Gärtner, 1915). Therefore, more efficient designs need to be developed that can replace the
67 simple orifice plates (Franke et al., 2011) or Venturi type constrictions (Zupanc et al., 2013),
68 which have considerable losses in pressure due to the severely restricted water flow.

Consequently, several new and innovative designs have been developed. Kumar and Pandit (1999) presented a design based on a high-speed homogenizer consisting of an impeller inside a cage-like stator with numerous slots which generates cavitation. It can generate cavitation of low intensity for the disruption of yeast cells (Kumar and Pandit, 1999). Moreover, Badve et al. (2013) presented a design that is based on a rotor and stator. The rotor is constructed of a solid cylinder with indentations on its surface within which strong shear forces are generated. It was successfully applied for wastewater treatment in wood finishing industry. Finally, a rotation generator was developed by Petkovšek et al. (2013) which is based on two facing rotors with special radial grooves where each one is spinning in the opposite direction. The geometry of the radial grooves is designed to form repeating pressure drops and rises. The generator has an advantage of low pressure losses, which makes it energy efficient and was successfully applied for waste-activated sludge disintegration (Petkovšek et al., 2013).

In our work we have cavitated two bacterial species *L. pneumophila* and *Escherichia coli* using a typical Venturi constriction and a rotation generator that is based on the previous design made by Petkovšek et al. (2013). In contrast to the previous design it is equipped with a rotor that has a new geometry for generating supercavitation (Dular et al., 2017). Microorganisms *L. pneumophila* and *E. coli* were chosen because of their potential to cause respiratory and gastrointestinal diseases in humans, respectively. Bacteria *L. pneumophila* (the cause of Legionnaries' disease) is a serious threat in warm water distributing systems, such as in hospitals, hotels or larger installations and prevention protocols are expensive and ineffective (Liu et al., 1998; Miller, 2012; Rota et al., 2004; Schulze-Röbbecke et al., 1987). Furthermore, toxic isolates of *E. coli* (Shiga strains) can cause life-threatening disease such as hemolytic-uremic syndrome (HUS) (Karmali, 1989) and recent outbreaks with high mortality rates are

92 becoming a serious concern for public health (Olsen et al., 2002). Additionally, because *E. coli* is
93 easy to use and quantify, it is routinely used as a faecal bioindicator for water samples (USEPA,
94 1986). Finally, the most potent cavitation treatment was also tested on bacteria *B. subtilis*, a
95 Gram positive bacterium that has a thicker peptidoglycan cell wall and is thus more resistant to
96 mechanical stress (Hayhurst et al., 2008).
97
98 **2 Experimental set-up and hydrodynamic conditions**
99 **2.1 Venturi type cavitation device**
100 The hydrodynamic cavitation test rig shown in Fig. 1, is made of a 3 L reservoir, heat exchanger
101 (to maintain the water temperature below 30°C), pump and a symmetrical Venturi section (Fig.
102 1, left).
103
104 The shape of the Venturi section enables us to establish various cavitation types (i.e. attached
105 steady cavitation, developed unsteady cavitation and supercavitation). The width of the section is
106 5 mm and at the throat the cross-section is 1 × 5 mm. The divergence angle of 10° was chosen on
107 the basis of previously established facts that unsteady cavitation forms optimally at this value
108 (Dular et al., 2012). The secondary divergence angle of 30° downstream was chosen to enable
109 the appearance of stabile supercavitation which needs more room to form. The section was
110 constructed of acrylic glass, which also enabled the observation of cavitation. Moreover, to
111 change the extent of cavitation, the flow velocity (rotational frequency of the pump) or the
112 system pressure were adjusted. The system pressure was adjusted in the partially filled reservoir
113 connected to a vacuum pump (a range of 0.1 bar to 6 bar).
114

2.2 Rotation generator of hydrodynamic cavitation

The rotation generator is based on the centrifugal pump design which has a modified rotor and a stator added in its housing. It was first constructed by Petkovšek et al. (2013). The rotation generator is made of an electric motor that propels the modified rotor. According to the axial direction of the pump, the stator's position is opposite to the modified rotor.

The stator and the surrounding housing are made of a transparent acrylic glass which enabled us to observe and photograph the cavitation process. This housed unit (with rotor and stator) forms the so-called cavitation treatment chamber. The structure of rotational generator still preserves its original flow-through pumping function, which makes its installation into the water pipe system simple with no additional pumping required.

In our experimental design, the rotation generator is installed in a model water system shown in Fig. 2. The model system is assembled from a 2 L reservoir, piping, heat exchanger, flow and pressure meters, and from the rotation generator. The piping and connections are made of standard household water system materials (ISO, 2003).

The modified rotor has a specially designed and patented geometry (Dular et al., 2017). The surface of the rotor consists of two symmetrical teeth, which are 14.8 mm wide, 4.15 mm high and their length stretches from 14.7 mm on the edges to 12.5 mm in the centre. Their shape has the same geometry as a symmetrical Venturi's lower or upper section (Fig. 3). The divergence angle of the teeth's cross section is 10° and the secondary divergence angle is 30° (Fig. 3). A lower or upper section of a typical symmetrical Venturi constriction has the same divergence angles (Fig. 1, right). These two teeth are based on a previously patented disk design (Sirok et al., 2016) that can generate large pressure pulsations and can be used to study the erosion of

different kinds of material. The surface of the added stator in our rotation generator is completely flat and the gaps between the tips of the teeth of the rotor and the stator's surface were set to be 1 mm. The space between the rotating tooth and the smooth surface of the stator resembles a Venturi constriction. The rotor's geometry forces the liquid to flow in a tangential and in a radial direction. Consequently, the tangential velocity of the liquid causes the liquid to circle in the treatment chamber while the radial velocity of the liquid causes further suction.

When the liquid in the treatment chamber is going through the tip of a tooth it is forced to accelerate and this causes a local drop in pressure. When the pressure falls below the evaporation pressure the liquid evaporates or cavitates. Moreover, there is enough room between the two teeth on the rotor that a large and stable supercavitation cavity can be formed there.

2.3 Hydrodynamics of hydrodynamic cavitation setup

Measurements of the system pressure (p), in the reservoir, were conducted upstream of the Venturi section using the Hygrosens DRTR-AL-10 V-R16B pressure probe (uncertainty of ±0.2%). Moreover, the evolution of the pressure that originates from hydrodynamic cavitation was measured using a hydrophone. These pressure fluctuations were measured in the treatment chamber or inside the Venturi section with a hydrophone Reson TC4013 with usable frequency range 1 Hz to 170 kHz and receiving sensitivity of -211 ± 3 dB re 1 V/µ Pa.

The flow rate was measured using the Buerkert SE32 flow meter (uncertainty of ±1%).

The temperature of the water sample was monitored by a PT100 A type resistance thermometer (uncertainty of ±0.2 K). On average, the pre- and post- treatment temperatures were 23.0 °C and 30.5 °C, respectively. The optimal growth temperature range for bacteria *E. coli* (Doyle and

Schoeni, 1984), *L. pneumophila* (Wadowsky et al., 1985) and *B. subtilis* (Curran and Evans, 1945) is around 35 °C – 37 °C. Therefore, the temperatures that were measured in our experiments had no negative effect on the viability of these bacterial species.

The Venturi type constriction, as well as rotation generator rotor and stator cover were made of transparent acrylic glass. This enabled us to film the cavitation clouds using a high-speed camera Photron SA-Z.

The cavitation number (σ) was calculated using the following equation:

$$\sigma = \frac{2\times(P_L - P_V)}{\rho \times v^2} \quad (1)$$

where P_V is the vapour pressure of water (3169 Pa at 25 °C); P_L is the locally measured pressure (Pa); v is the characteristic flow velocity (m/s); and ρ is the density of water (1000 kg/m3 at 25 °C) (Franc, 2006).

2.4 Microbiological measurements

2.4.1 Strains and sample preparation

L. pneumophila, subsp. *pneumophila* ATCC 33153 acquired from the Czech Collection of Microorganisms (CCM), *E. coli* strain MG 1655, DE3 resistant to kanamycin, and *B. subtilis* strain PS216 were used in the study. *E. coli*, *L. pneumophila* and *B. subtilis* were cultured at 37 °C on Luria broth agar plates (LB; 1.5 % agar), on buffered charcoal yeast extract agar plates (BCYE) and on LB agar plates (LB; 2.0 % agar), respectively. LB agar medium was composed

184 of 20 g/L of Luria agar broth (15 g/L (1.5 %) or 20 g/L (2.0 % for *B. subtilis*) of agar, 10g/L of
185 tryptone, 10g/L of NaCl and 5g/L of yeast extract, Sigma-Aldrich), and when the medium was
186 used for *E. coli* it was additionally supplemented with 50 µg/mL kanamycin sulphate (KM)
187 (Sigma-Aldrich). BCYE agar was composed of yeast extract 10 g/L (Difco), charcoal activated
188 2.0 g/L (Sigma), ACES buffer 10.0 g/L (Sigma), α-ketoglutarate monopotassium salt 1.0 g/L
189 (Sigma), ferric pyrophosphate 250 mg/l (Sigma), L-cysteine hydrochloride 400 mg/l (Sigma),
190 and agar 13 g/L (Difco) with pH set to 6.9 ± 0.2.
191
192 For the hydrodynamic cavitation experiments one colony of either *E. coli*, *L. pneumophila* or *B.*
193 *subtilis* were transferred into an Erlenmeyer flask containing 100 mL of appropriate liquid
194 medium (the above-mentioned culture media with the omission of agar) and were incubated
195 overnight in the dark, at 37 °C, 200 rpm. Next, the *L. pneumophila* test sample was prepared by
196 diluting the overnight culture in saline solution (0.9 % NaCl) to a concentration of around 1.1 x
197 10^6 CFU/mL and was stored on ice in a Styrofoam box to prevent temperature or UV rays to
198 affect the concentration of *L. pneumophila*. Just before the experiment, the test sample was
199 further diluted in tap water to a final concentration of $1.0 \cdot 10^5$ CFU/mL. When the overnight
200 culture of *E. coli* reached an OD_{650} (optical density at 650 nm) of around 1.8, it was diluted 5
201 times and was stored on ice in a Styrofoam box. Just before the experiment, it was further diluted
202 10 times to a final concentration of around $1.0 \cdot 10^8$ CFU/mL. When *B. subtilis* was used, an
203 overnight culture with OD_{650} 1.7 was diluted 5 times and was again stored on ice. Before the
204 cavitation run, the culture was further diluted 100 times to a final concentration of around $1.0 \cdot 10^5$
205 CFU/mL.

206 The sample volume for the Venturi setup, for all bacterial species, was 4 L and for the rotation
207 generator it was 2 L.
208
209 **2.4.2 Sampling and quantification**
210 During sampling, 40 ml of water were released from the device through the sampling valve and
211 poured back into the cavitation device through the entry valve. This ensured that a trapped dead
212 volume inside the sampling pipe that was not cycled through the cavitation device was not
213 analysed. Next, 10 mL of the sample was taken and was stored in 50 mL tubes on ice in a
214 Styrofoam box. The impact of hydrodynamic cavitation on the destruction of bacteria was
215 monitored by colony counts. For this, samples of 100 µL were plated on LB agar medium (1.5 %
216 agar) supplemented with 50 µg/mL of KM (for *E. coli*), or on LB agar medium (2.0 % agar)
217 without antibiotics (for *B. subtilis*) or on BCYE medium (for *L. pneumophila*) using the
218 successive dilution method in saline solution. Colonies were counted after an overnight
219 incubation at 37 °C and results were expressed in $\log_{10}$CFU/mL. All values reported in this paper
220 are the mean of at least two independent biological treatments and three replicates for each
221 treatment. The average values and standard errors are given.
222
223 To evaluate the impact of cavitation on the overall growth reduction, a specific decay rate
224 constant (µ) was calculated as follows:
225
226 $$\mu = \frac{ln\, X_f - ln\, X_0}{t_f - t_0} \quad (2)$$
227

228 Specific decay rate (1/h) is the slope of the microbial growth curve and is negative when cells
229 start dying (Maier, 2009). X_0 is colony count per millilitre at the beginning of treatment; X_f is
230 colony count per millilitre at the end of treatment; t_0 is time at the beginning of treatment and t_f is
231 time at the end of treatment.
232
233 Safety precautions for working with *E. coli* and *L. pneumophila* and their quantification were in
234 accordance with the (ISO, 1998). *B. subtilis* is a non-pathogenic microorganism and is used in
235 probiotics.
236
237 To ensure that the hydrodynamic device (Venturi or rotational generator) was free of
238 microorganisms, before and after each hydrodynamic cavitation experiment, the device was
239 cleaned using a washing protocol. This consisted of one rinse with tap water (running the
240 hydrodynamic cavitation device filled with tap water for 5 min), next 15 min of running the
241 device with 5 % (v/v) sodium dodecyl sulphate (sigma, USA), and finally with six successive
242 device volume rinses with tap water (each lasting 5 min). The rinse water was disposed after an
243 overnight exposure to active chlorine.
244
245 **3 Results**
246 **3.1 Analysis of cavitation conditions**
247 **3.1.1 The Venturi section setup**
248 To establish the attached steady cavitation, the upstream absolute pressure was maintained at 6
249 bar and the flow velocity at the throat of the Venturi section was 27.6 m/s (cavitation number σ
250 was 1.57; calculated according to Šarc et al. (2016)) (Table 1). In these conditions, a 4 L water

sample took 0.5 min to complete one pass through the Venturi section (flow rate Q of 8.2 L/min). The developed hydrodynamic cavitation was established at 5 bar and 27.6 m/s (cavitation number was 1.31). Supercavitation was established at 0.2 bar and 6.7 m/s (flow rate of 2 L/min; cavitation number of 0.78) and one sample pass (4 L) was completed in 2 min.

The flow conditions in the Venturi constriction are presented in Fig. 4. The image sequences (images from 1 to 5) were recorded by a high-speed camera and are approximately 6 ms long. On the images, water flows from the left to the right side of the Venturi section. The attached steady cavitation sequence is shown in the left panel, developed cavitation is given in the middle, and supercavitation is represented in the right panel sequence.

The diagrams at the bottom of Fig. 4 show the evolution of the pressure measured using a hydrophone inside the Venturi section. As expected we see larger fluctuations in the case of developed cavitation, while the initial cavitation and the supercavitating flows do not cause significant pressure perturbations.

The attached steady cavitation filled up the whole flow cross-section and extended approximately 10 mm along the Venturi section (Fig. 4, left sequence). No separations of cavitation clouds were visible; hence no larger pressure fluctuations were expected at these conditions. In the case of developed cavitation (Fig. 4, middle sequence) the dynamics of bubble formation was more pronounced. One can see an attached part of the cavitation cloud which extends from the throat of the Venturi section to approximately 20 mm downstream of the section. At the end of the attached cavity large bubbles and bubble clusters were shed. These

were carried by the flow into a region of higher-pressure where they violently collapsed. When supercavitation was observed (the right sequence in Fig. 4), the Venturi section was completely filled with one large and stable vapour cavity with a number of small bubbles forming at the upper part of this cavity.

Table 1: Hydrodynamic cavitation characteristics of initial cavitation, developed cavitation and supercavitation.

3.1.2 Rotational cavitation generator

Figure 5 shows the operational characteristics of the rotation generator at its maximal rotation frequency of 9025 min^{-1}. The image sequences were recorded by a high-speed camera and follow a series of five 0.2 ms long time steps. The rotor is moving in a counter clockwise direction. On the left side of Figure 5 there is a diagram that shows the dependence of flow rate to the head (H) of the pump and on the right side of the figure, these conditions were photographed. At flow rate of 5 L/min and at head of 7.6 m (point A, panel A), the generator is operating in non-cavitating conditions. According to the images, the initial cavitation is formed when the flow rate reaches 4 L/min (head pump of 8 m) (point B, panel B). The images clearly show small and attached cavities that begin from the tips of both teeth and stretch no more than 9 mm in length. When the flow rate is lowered to 1.8 L/min (head of 9.8 m), the cavitation becomes developed and shedding and collapsing of cavitation clouds can be seen (point C, panel C). Bubbles are formed at the tip of the tooth and are shed around 20 mm behind the tip. Finally, if the flow rate is only 0.2 L/min (H of 10 m), supercavitation develops and one large and stable vapour cavity fills the entire volume behind the tooth of the rotor (panel D).

For the attached steady cavitation, developed cavitation and for supercavitation a single sample pass (2 L) was completed in 0.5 min, 1.1 min and in 10 min, respectively.

3.2 Influence of cavitation on the destruction of bacteria

3.2.1 Venturi section setup

The effect of cavitation, developed in the Venturi constriction, on the destruction of bacteria *E. coli* and *L. pneumophila* is presented in Fig. 6. After the first 27 cavitation passes through the section attached steady cavitation/initial cavitation did not significantly impact the colony count of *E. coli* (Fig. 6A). Similar observations were made when the initial cavitation was tested on the bacteria *L. pneumophila* (Fig. 6B). Moreover, the impact of developed cavitation on these two species of bacteria was also insignificant (Fig. 6).

However, when supercavitation was studied, the destruction was statistically significant for both species. For bacteria *E. coli* the viable count linearly decreased and was reduced to 7.3 $Log_{10}CFUmL^{-1}$ after 60 cavitation passes (Fig. 6A). After 60 passes the initial *E. coli* concentration of 7.9 $Log_{10}CFUmL^{-1}$ was reduced for 0.6 logs (a reduction of 75.40 %).

For bacteria *L. pneumophila*, the viable count was lowered to 4.6 $Log_{10}CFUmL^{-1}$ during the first 10 supercavitation passes. After that, the reduction of its viable count increased and after 30 cavitation passes the viable count was down to 2.7 $Log_{10}CFUmL^{-1}$ (Fig. 6B). According to these measurements, a reduction of 2.1 logs was achieved after 30 cavitation passes (99.30 % reduction of the initial concentration of 4.92 $Log_{10}CFUmL^{-1}$).

3.2.2 Rotational cavitation generator

The effect of the new rotation generator on the destruction of bacteria *E. coli*, *L. pneumophila* and *B. subtilis* is presented in Fig. 7. Similarly, to the Venturi setup, the initial cavitation and the developed cavitation that were formed inside the rotation generator did not significantly influence the viable count of bacteria *E. coli* (Fig. 7A). On the other hand, the supercavitation treatment was very effective, and the colony count of *E. coli* was reduced to 4.8 $Log_{10}CFUmL^{-1}$ after 15 cavitation passes (Fig.7A). According to the initial *E. coli* concentration of 8.1 $Log_{10}CFUmL^{-1}$, a reduction of 3.3 logs was achieved (99.95 % reduction) (Table 2).

Because the attached steady and the developed cavitation types in the rotation generator were not effective for the eradication of bacteria *E. coli,* similarly to the Venturi system, we assumed that the attached steady and the developed cavitation, generated inside the rotation generator, would also have no impact on the bacteria *L. pneumophila.* Therefore, for the rotation generator experiments, we have decided that *L. pneumophila* and *B. subtilis* will only be treated by supercavitation.

In Fig. 7B the destruction of bacteria *L. pneumophila* using supercavitation is presented. After the first 5 min of the experiment, inside the rotation generator, the viable count decreased rapidly and after 6 cavitation passes (60 min of operation) it fell to 2.2 $Log_{10}CFUmL^{-1}$. Therefore, the initial *L. pneumophila* concentration of 5.8 $Log_{10}CFUmL^{-1}$ was reduced by 3.6 logs (a reduction of 99.98 %) (Table 2).

To test if supercavitation treatment is effective against Gram positive bacteria that have a thicker cell wall and are thus more physically stable to Gram negative bacteria, *B. subtilis* was supercavitated for 120 min using the rotation generator (Fig. 7B). After the first 3 cavitation passes (30 min of operation) only a slight reduction was observed, however later the effectiveness improved and after 6 cavitation passes (60 min of operation) the viable count was reduced to 3.9 $Log_{10}CFUmL^{-1}$ (a reduction of 95.69 %). A further drop in colony count was measured after 60 min of cavitation and towards the end of the experiment the viable count was down to only 1.4 $Log_{10}CFUmL^{-1}$. According to the initial *B. subtilis* concentration of 5.3 $Log_{10}CFUmL^{-1}$, a strong reduction of 3.8 logs was achieved (a reduction of 99.98 %) after 12 cavitation passes (120 min of operation) (Table 2).

3.2.3 Economic evaluation

In terms of economic feasibility, one can refer to the work of Bolton et al. (2001), who introduced a figure of merit "Electric energy per order of reduction (E_{EO})". This is the amount of electric energy that is required to bring the bacterial count down by one order of magnitude. The E_{EO} value in kWh/m^3/order can be calculated as follows:

$$E_{EO} = \frac{P}{Q \cdot Log_{10}CFU} \quad (3)$$

where P is the rated power (kW) of the system, Q is the volume flow rate (m^3/h) and $log_{10}CFU$ is the logarithmic reduction in colony count. During the experiments, the cavitation generator used approximately 280 W of power, while the pump that drove the flow through Venturi section required roughly 1 kW (regardless of the operating point). Higher E_{EO} values correspond to lower

364 removal efficiencies. Table 3 shows the average E_{EO} values and approximate costs for each
365 cavitation type.
366
367 **4 Discussion**
368 In this work, we first studied the development of 3 different types of cavitation that were
369 generated inside the Venturi setup or inside the rotation generator. When using different flow
370 velocities and/or different system pressures, Venturi setup generated the attached steady
371 cavitation, the developed cavitation or the supercavitation as demonstrated with a high-speed
372 camera. The steady cavitation was attached and cloud separation was not visible. The developed
373 cavitation was dynamic and consisted of bubble shedding and of bubble collapse. Finally, a
374 constant and large supercavitation cavity that filled up the whole Venturi section and smaller
375 bubbles above this cavity were observed. The visual data were also backed up with hydrophone
376 pressure measurements that showed larger pressure fluctuations only in the case of the developed
377 cavitation (Figure 4).
378
379 The typical characteristics of the three mentioned types of hydrodynamic cavitation were also
380 observed in the rotation cavitation generator. Behind the tip of the tooth of the spinning rotor, the
381 attached steady cavitation formed small cavities, whereas the developed cavitation was
382 accompanied by bubble cloud shedding. For supercavitation, the entire section behind the tooth's
383 tip was engulfed within a single vapour cavity.
384
385 The three types of cavitation were tested for their antimicrobial potential. For the Venturi section
386 setup, the attached steady and the developed cavitations did not significantly reduce the viable

387 counts of bacteria *E. coli* and *L. pneumophila*. However, when supercavitation was applied, the
388 *E. coli* and the *L. pneumophila* viable counts were reduced by 0.6 logs (a 75.40 % reduction after
389 60 passes; $\mu = -0.69$)) and by 2.1 logs (a 99.30 % reduction after 30 passes; $\mu = -5.07$),
390 respectively (Table 2).
391
392 As supercavitation is not associated with the generation of pressure pulses, high shear forces,
393 high local temperatures or OH^- reactive radicals, it is generally recognized as non-aggressive
394 (Dommerich et al., 2012). Consequently, this method is not considered to be effective against
395 bacteria or against other microorganisms. Although the results of this study are surprising, they
396 are consistent with the findings of Šarc et al. (2016) where supercavitation was far more efficient
397 than the developed cavitation.
398
399 The reason for the potency of supercavitation could lie in cavity structure. As the flow reaches
400 the constriction section of the Venturi, it enters the large supercavitation cavity. In the transition
401 from the liquid to the vapour phase, the pressure drop is almost instantaneous (an instantaneous
402 evaporation occurs). According to model, the bacterial cells are most probably damaged when
403 they enter the large supercavitation cavity and rapidly expose themselves to a very low pressure
404 inside the cavity (Šarc et al., 2016). This instantaneous pressure decrease, may disrupt the
405 bacteria (Dommerich et al., 2012). If the flow rate and the size of the Venturi section are
406 considered, the transition from the liquid to the vapour phase occurs in an order of just a few
407 milliseconds. This transition is probably quick enough to cause the irreversible cell damage.
408 Moreover, the sudden pressure increase at the end of the large supercavitation cavity, could also
409 add to the bacterial disruption.

410

411 Similar physical mechanism for bacteria disruption was also envisaged in nitrogen
412 decompression reservoirs (Hemmingsen & Hemmingsen 1978; Gottlieb & Adachi 2000). Here
413 large quantities of nitrogen are dissolved in a water sample and the water sample is then tightly
414 sealed within the reservoir. As soon as the reservoir is opened, the sudden difference in pressure
415 results in the formation of forces that can disrupt cell membranes. Moreover, the proposed
416 mechanism is also supported by the functional principle of a French pressure cell press (French,
417 2007). In a French press, the pressure is suddenly released through a valve into the surrounding
418 area and the sudden pressure drop rapidly depressurizes the bacteria. These devices are routinely
419 used in biological experimentation to disrupt the plasma membrane of cells, however, they are
420 only suitable for small volume batch mode applications (up to 30 mL).
421

422 The exact mechanism of supercavitation by which the bacterial cells are disrupted during the
423 sudden pressure decrease is currently unknown. Nevertheless, the sole pressure shock (that is
424 generated during the rapid pressure drop in the transition area between liquid and vapour) could
425 cause a burst in the cell membrane. It was shown by Ganzenmüller et al. (2011) that the lipid
426 bilayer membrane can be irreversibly damaged when the shock waves travel through its surface.
427

428 Furthermore, when the rotation generator was applied, the initial and developed cavitations again
429 proved to be ineffective. On the other hand, supercavitation that was developed inside the
430 rotation generator reached reductions of 3.3 logs (99.95 % reduction after 15 cavitation passes
431 (150 min); $\mu = -3.04$), 3.6 logs (99.98 % reduction after 6 cavitation passes (60 min); $\mu = -8.29$)

and 3.8 logs (99.98 % reduction after 12 cavitation passes (120 min); $\mu = -4.49$) for bacteria *E. coli, L. pneumophila* and *B. subtilis,* respectively (Table 2).

For similar supercavitation treatment times, the disruption of bacteria *E. coli* was 4.2 times more efficient in the rotation generator (2.5 logs reduction) in comparison to the Venturi setup (0.6 logs reduction). Moreover, a 1.7 times greater efficiency of the rotation generator was also observed for the bacteria *L. pneumophila* (a 2.1 logs reduction in the Venturi setup and a 3.6 logs reduction in the rotation generator). Furthermore, when we compare the efficiencies of the two devices after 15 supercavitation passes, the superiority of the rotation generator for bacteria *E. coli* is undeniable (21.4 times greater efficiency). Additionally, after 6 supercavitation passes, a 15.9 times greater efficiency of the rotation generator is achieved for bacteria *L. pneumophila.*

Therefore, our experimental results show that, we have designed and manufactured a new rotational hydrodynamic cavitation device that is far more efficient in comparison to the Venturi cavitation device.

The greater efficiency of the rotation generator could be its ability to generate greater shear forces which are caused by the rotation of the teeth of the rotor and the rotation of liquid that is located between the rotor and the stator (tangential velocity of the liquid causes the liquid to circle) (Franc and Michel, 2004; Petkovšek et al., 2015, 2013). Furthermore, when compared with the usual orifice plates or with the Venturi sections, the rotation generator is more energy efficient, because it has significantly lower losses of pressure (Franke et al., 2011; Zupanc et al., 2013). Additionally, because an orifice plate consists of small holes, there is a high risk of permanent obstruction development. Finally, the rotor of the rotation generator is designed in a

455 way that causes further suction of liquid (generated by the liquids radial velocities) and is
456 therefore independent of any additional pumping.
457
458 From the economic evaluation we can see that the rotation generator which operates in the
459 supercavitating regime surpasses all other devices for water treatment (Table 3). Also, in
460 comparison to conventional techniques, such as introduction of thermal shocks, the presented
461 method is much better in terms of power consumption. A typical thermal shock requires
462 approximately 30 kWh/m^3/order (Šarc et al., 2016).
463
464 Because a small number of supercavitation passes is needed to achieve 3.6 logs reduction rates of
465 bacteria *L. pneumophila*, the rotation generator seems ideal for continuous water installations and
466 for larger industrial applications. Furthermore, it enables the treatment of entire volumes of
467 water, which is especially important for the areas that are susceptible to *L. pneumophila*
468 contaminations.
469
470 **5 Conclusions**
471 In this work we present a new rotation cavitation generator with a newly designed rotor that
472 efficiently eliminates Gram negative (*L. pneumophila*, *E. coli*) as well as Gram positive (*B.*
473 *subtilis*) bacteria. The main mode of antibacterial action is not the developed cavitation, which is
474 known to be aggressive for bacteria. On the contrary, the highest antibacterial effect was
475 observed with supercavitation where a mixture of supercavitation and high shear forces disrupts
476 bacterial cells within the treated volumes. We believe that a 3.6 logs reduction of the bacteria *L.*

pneumophila in the rotational cavitation generator is a great improvement over the usual Venturi type setups.

6 References

Badve, M., Gogate, P., Pandit, A., Csoka, L., 2013. Hydrodynamic cavitation as a novel approach for wastewater treatment in wood finishing industry. Sep. Purif. Technol. 106, 15–21. doi:10.1016/j.seppur.2012.12.029

Bolton, J.R., Bircher, K.G., Tumas, W., Tolman, C.A., 2001. Figures-of-merit for the technical development and application of advanced oxidation technologies for both electric- and solar-driven systems (IUPAC Technical Report). Pure Appl. Chem. 73, 627–637. doi:10.1351/pac200173040627

Curran, H.R., Evans, F.R., 1945. Heat Activation Inducing Germination in the Spores of Thermotolerant and Thermophilic Aerobic Bacteria. J. Bacteriol. 49, 335–46.

Dommerich, S., Frickmann, H., Ostwald, J., Lindner, T., Zautner, A.E., Arndt, K., Pau, H.W., Podbielski, A., 2012. Effects of high hydrostatic pressure on bacterial growth on human ossicles explanted from cholesteatoma patients. PLoS One 7, e30150. doi:10.1371/journal.pone.0030150

Doyle, M.P., Schoeni, J.L., 1984. Survival and growth characteristics of Escherichia coli associated with hemorrhagic colitis. Appl. Environ. Microbiol. 48, 855–6.

Dular, M., Griessler-Bulc, T., Gutierrez-Aguirre, I., Heath, E., Kosjek, T., Krivograd Klemenčič, A., Oder, M., Petkovšek, M., Rački, N., Ravnikar, M., Šarc, A., Širok, B., Zupanc, M., Žitnik, M., Kompare, B., 2016. Use of hydrodynamic cavitation in (waste)water treatment. Ultrason. Sonochem. 29, 577–588. doi:10.1016/j.ultsonch.2015.10.010

500 Dular, M., Khlifa, I., Fuzier, S., Adama Maiga, M., Coutier-Delgosha, O., 2012. Scale effect on
501 unsteady cloud cavitation. Exp. Fluids 53, 1233–1250. doi:10.1007/s00348-012-1356-7
502 Dular, M., Sarc, A., Stopar, D., Kosel, J., 2017. Generator of supercavitation for bacteria
503 destruction in water. Slovenian patent office, P-201700058.
504 Exner, M., Vacata, V., Gebel, J., 2003. Heterotrophic plate counts and drinking-water safety, in:
505 Bartram, J., Cotruvo, J. A., Exner, M., Fricker, C., & Glasmacher, A. (Ed.), . IWA
506 publishing.
507 Franc, J.-P., 2006. Physics and Control of Cavitation.
508 Franc, J.-P., Michel, J.-M., 2004. Fundamentals of cavitation. Kluwer Academic Publishers.
509 Franke, M., Braeutigam, P., Wu, Z.-L., Ren, Y., Ondruschka, B., 2011. Enhancement of
510 chloroform degradation by the combination of hydrodynamic and acoustic cavitation.
511 Ultrason. Sonochem. 18, 888–894. doi:10.1016/j.ultsonch.2010.11.011
512 French, 2007. FRENCH ® Press Operation Manual.
513 Ganzenmüller, G.C., Hiermaier, S., Steinhauser, M.O., Chand, D., Vries, A.H. de, 2011. Shock-
514 wave induced damage in lipid bilayers: a dissipative particle dynamics simulation study.
515 Soft Matter 7, 4307. doi:10.1039/c0sm01296c
516 Gärtner, A., 1915. Die Hygiene des Wassers. Springer Vieweg.
517 Gogate, P.R., Pandit, A.B., 2004. Sonochemical reactors: scale up aspects. Ultrason. Sonochem.
518 11, 105–117. doi:10.1016/j.ultsonch.2004.01.005
519 Gottlieb, R.A., Adachi, S., 2000. Nitrogen cavitation for cell disruption to obtain mitochondria
520 from cultured cells. Methods Enzymol. 322, 213–21.
521 Hayhurst, E.J., Kailas, L., Hobbs, J.K., Foster, S.J., 2008. Cell wall peptidoglycan architecture in
522 Bacillus subtilis. Proc. Natl. Acad. Sci. U. S. A. 105, 14603–8.

523 doi:10.1073/pnas.0804138105
524 Hemmingsen, B.B., Hemmingsen, E.A., 1978. Tolerance of bacteria to extreme gas
525 supersaturations. Biochem. Biophys. Res. Commun. 85, 1379–84.
526 Hulsmans, A., Joris, K., Lambert, N., Rediers, H., Declerck, P., Delaedt, Y., Ollevier, F., Liers,
527 S., 2010. Evaluation of process parameters of ultrasonic treatment of bacterial suspensions
528 in a pilot scale water disinfection system. Ultrason. Sonochem. 17, 1004–1009.
529 doi:10.1016/j.ultsonch.2009.10.013
530 ISO, 2003. ISO 15874-3:2003 - Plastics piping systems for hot and cold water installations --
531 Polypropylene (PP) -- Part 3: Fittings [WWW Document].
532 ISO, 1998. ISO 11731:1998 - Water quality -- Detection and enumeration of Legionella [WWW
533 Document].
534 Karmali, M.A., 1989. Infection by verocytotoxin-producing Escherichia coli. Clin. Microbiol.
535 Rev. 2, 15–38.
536 Kumar, P.S., Pandit, A.B., 1999. Modeling Hydrodynamic Cavitation. Chem. Eng. Technol. 22,
537 1017–1027. doi:10.1002/(SICI)1521-4125(199912)22:12<1017::AID-
538 CEAT1017>3.0.CO;2-L
539 Liu, Z., Stout, J.E., Boldin, M., Rugh, J., Diven, W.F., Yu, V.L., Yu, V.L., Wadowsky, R.M.,
540 1998. Intermittent Use of Copper- Silver Ionization for Legionella Control in Water
541 Distribution Systems: A Potential Option in Buildings Housing Individuals at Low Risk of
542 Infection. Clin. Infect. Dis. 26, 138–140. doi:10.1086/516283
543 Maier, R., 2009. Bacterial Growth, in: Maier, R., Pepper, I., Gerba, C. (Eds.), Environmental
544 Microbiology. Academic press, pp. 37–40.
545 Mezule, L., Tsyfansky, S., Yakushevich, V., Juhna, T., 2009. A simple technique for water

disinfection with hydrodynamic cavitation: Effect on survival of Escherichia coli. Desalination 248, 152–159. doi:10.1016/j.desal.2008.05.051

Miller, R.S., 2012. A Review of Common Disinfection Techniques and What ASHRAE Proposed 188P. Am. Soc. Sanit. Eng. Plumbing S, 12–15.

Olsen, S.J., Miller, G., Breuer, T., Kennedy, M., Higgins, C., Walford, J., McKee, G., Fox, K., Bibb, W., Mead, P., 2002. A waterborne outbreak of Escherichia coli O157:H7 infections and hemolytic uremic syndrome: implications for rural water systems. Emerg. Infect. Dis. 8, 370–5. doi:10.3201/eid0804.000218

Petkovšek, M., Mlakar, M., Levstek, M., Stražar, M., Širok, B., Dular, M., 2015. A novel rotation generator of hydrodynamic cavitation for waste-activated sludge disintegration. Ultrason. Sonochem. 26, 408–414. doi:10.1016/j.ultsonch.2015.01.006

Petkovšek, M., Zupanc, M., Dular, M., Kosjek, T., Heath, E., Kompare, B., Širok, B., 2013. Rotation generator of hydrodynamic cavitation for water treatment. Sep. Purif. Technol. 118, 415–423. doi:10.1016/j.seppur.2013.07.029

Riesz, P., Kondo, T., 1992. Free radical formation induced by ultrasound and its biological implications. Free Radic. Biol. Med. 13, 247–70.

Rota, M.C., Caporali, M.G., Massari, M., European Working Group for Legionella Infections, 2004. European Guidelines for Control and Prevention of Travel Associated Legionnaires' Disease: the Italian experience. Euro Surveill. 9, 10–1.

Šarc, A., Oder, M., Dular, M., 2016. Can rapid pressure decrease induced by supercavitation efficiently eradicate Legionella pneumophila bacteria? http://dx.doi.org/10.1080/19443994.2014.979240 57, 2184–2194.

Schulze-Röbbecke, R., Rödder, M., Exner, M., 1987. Multiplication and killing temperatures of

naturally occurring legionellas. Zentralbl. Bakteriol. Mikrobiol. Hyg. B. 184, 495–500.

Sirok, B., Dular, M., Petkovsek., M., 2016. Cavitation Device. US Patent Office, 15/049,409.

Stinebring, D.R., Billet, M.L., Lindau, J.W., Kunz, R.F., 2001. Developed Cavitation-Cavity Dynamics.

USEPA, 1986. Ambient water quality criteria for bacteria. United States Environ. Prot. AgencyEPA 440/5-84-002, January.

von Eiff, C., Overbeck, J., Haupt, G., Herrmann, M., Winckler, S., Richter, K.D., Peters, G., Spiegel, H.U., 2000. Bactericidal effect of extracorporeal shock waves on Staphylococcus aureus. J. Med. Microbiol. 49, 709–12. doi:10.1099/0022-1317-49-8-709

Wadowsky, R.M., Wolford, R., McNamara, A.M., Yee, R.B., 1985. Effect of temperature, pH, and oxygen level on the multiplication of naturally occurring Legionella pneumophila in potable water. Appl. Environ. Microbiol. 49, 1197–205.

Zupanc, M., Kosjek, T., Petkov?ek, M., Dular, M., Kompare, B., ?irok, B., Bla?eka, ?eljko, Heath, E., 2013. Removal of pharmaceuticals from wastewater by biological processes, hydrodynamic cavitation and UV treatment. Ultrason. Sonochem. 20, 1104–1112. doi:10.1016/j.ultsonch.2012.12.003

587 **Figure Captions**

588

589 Fig.1: Scheme of the test-rig (left) and the Venturi section (right).

590

591 Fig. 2: Scheme of a model water system and the rotating cavitation generator (left). The main
592 parts of the rotation generator are: electromotor (1), rotor blade (2), front (3) and back housing
593 (4) (Dular et al., 2017).

594

595 Fig. 3: Geometry of the rotor of the rotation cavitation generator (Dular et al., 2017).

596

597 Fig. 4: Cavitation types in the Venturi type cavitation device, attached steady cavitation (left),
598 developed cavitation (middle) and supercavitation (right)). The bottom diagrams show the
599 pressure evolution measured inside the Venturi section.

600

601 Fig. 5: Hydrodynamic characteristic of the generator and the appearances of cavitation at
602 different operating conditions.

603

604 Fig. 6: Destruction of bacteria *E. coli* (A) and *L. pneumophila* (B) by attached steady cavitation,
605 developed cavitation and supercavitation in a Venturi type section.

606

607 Fig. 7: The influence of hydrodynamic cavitation generated inside the rotation generator on
608 different species of bacteria. (A): Removal of bacteria *E. coli,* using the initial, the developed

609 cavitation and the supercavitation; (B): Removal of bacteria *E. coli, L. pneumophila* and *B.*

610 *subtilis* using supercavitation.

611

612 **Table Captions**

613

614 Tab. 1: Hydrodynamic cavitation characteristics of initial cavitation, developed cavitation and

615 supercavitation.

616

617 Tab. 2: The effect of supercavitation, generated in the Venturi section setup and in the rotation

618 generator, on the destruction of Gram negative and Gram positive bacteria.

619

620 Tab. 3: Electrical efficiency of each investigated cavitation type.

Table01

	Local pressure (P_L) (Pa)	Characteristic flow velocity (v) (m/s)	Cavitation number (σ)
Initial cavitation	600000	27.6	1.57
Developed cavitation	500000	27.6	1.31
Supercavitation	20000	6.7	0.78

Table02

	$Log_{10} X_0$ ($Log_{10}CFUmL^{-1}$)	$Log_{10} X_f$ ($Log_{10}CFUmL^{-1}$)	Number of cavitation passes	t_f (h)	Log reduction	Reduction rate (%)	μ (from t_0 to t_f) (1/h)
Venturi section setup							
E. coli	7.9	7.3	60	2	0.6	75.40	-0.69
L. pneumophilla	4.9	2.7	30	1	2.1	99.30	-5.07
Rotation generator							
E. coli	8.1	4.8	15	2.5	3.3	99.95	-3.04
B. substilis	5.3	1.4	12	2	3.8	99.98	-4.49
L. pneumophilla	5.8	2.2	6	1	3.6	99.98	-8.29

Abbervations: μ is specific decay rate constant; X_0 is $CFUmL^{-1}$ at the beginning of treatement; X_f is $CFUmL^{-1}$ at the end of treatement; t_0 is time at the beginning of treatement (always 0 h) and tf is time at the end of treatement.

Table03

E_{EO} (kWh/m^3/order)	Venturi		Rotation generator		
	E. coli	*L. pneumophila*	*E. coli*	*L. pneumophila*	*B. subtilis*
Initial cavitation	20.83	18.75	9.33	/	/
Developed cavitation	43.75	38.19	8.17	/	/
Supercavitation	6.94	0.99	0.04	0.01	0.02

Figure 01
Click here to download high resolution image

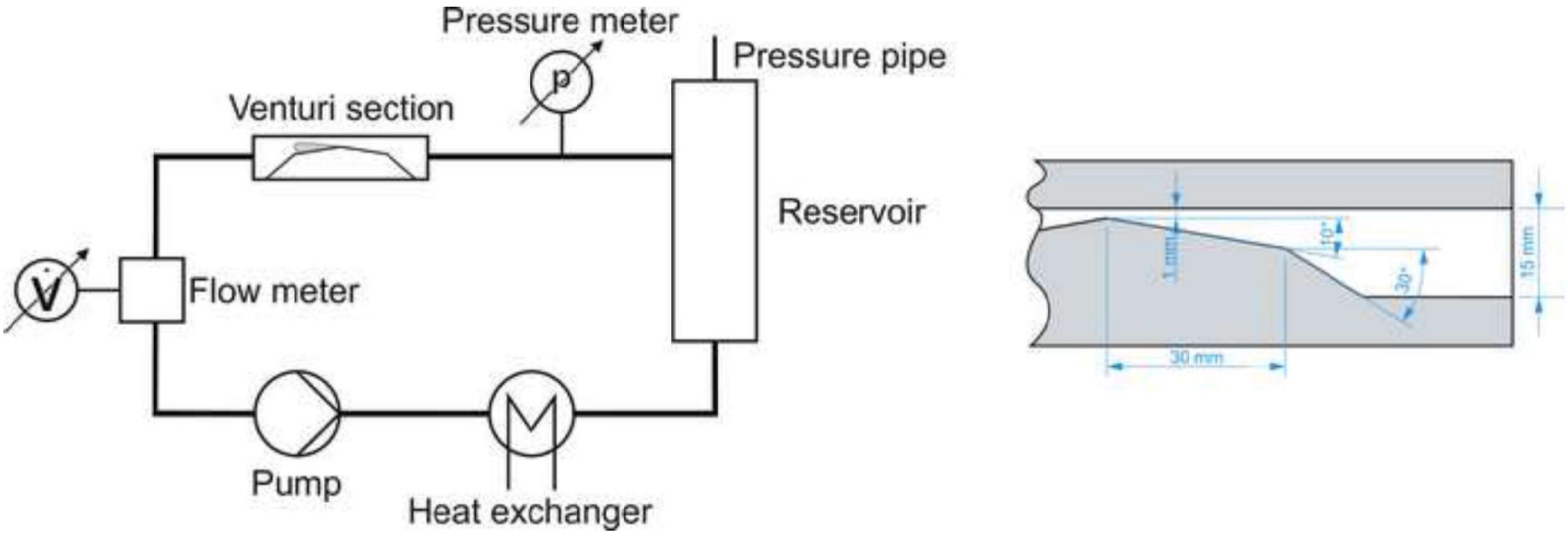

Figure 02
Click here to download high resolution image

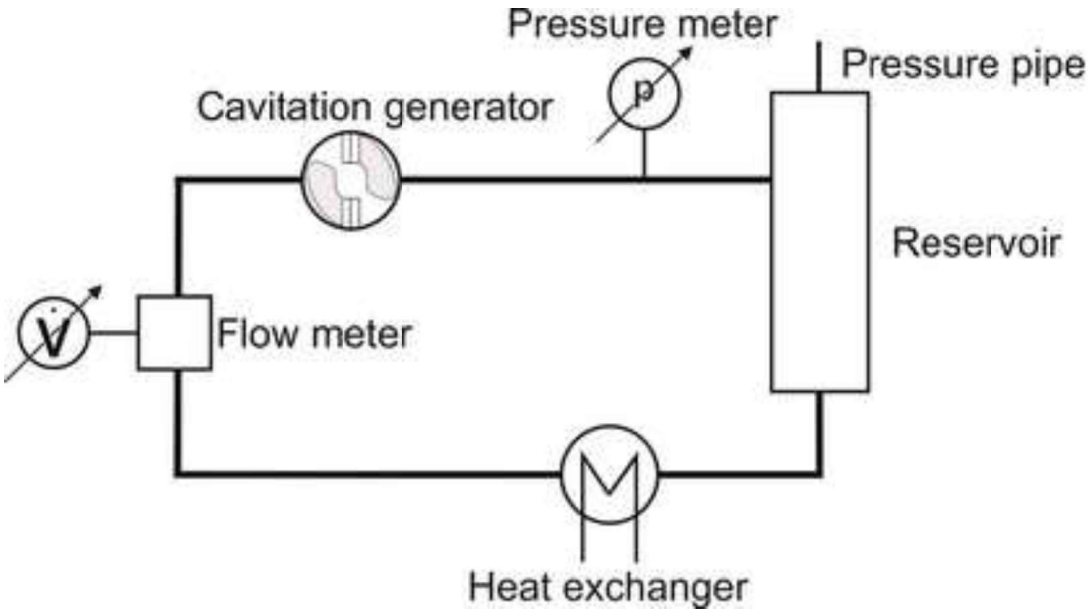

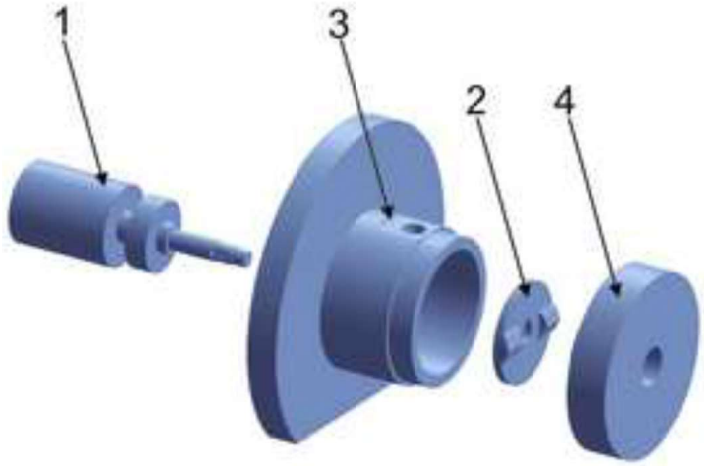

Figure 03

Click here to download high resolution image

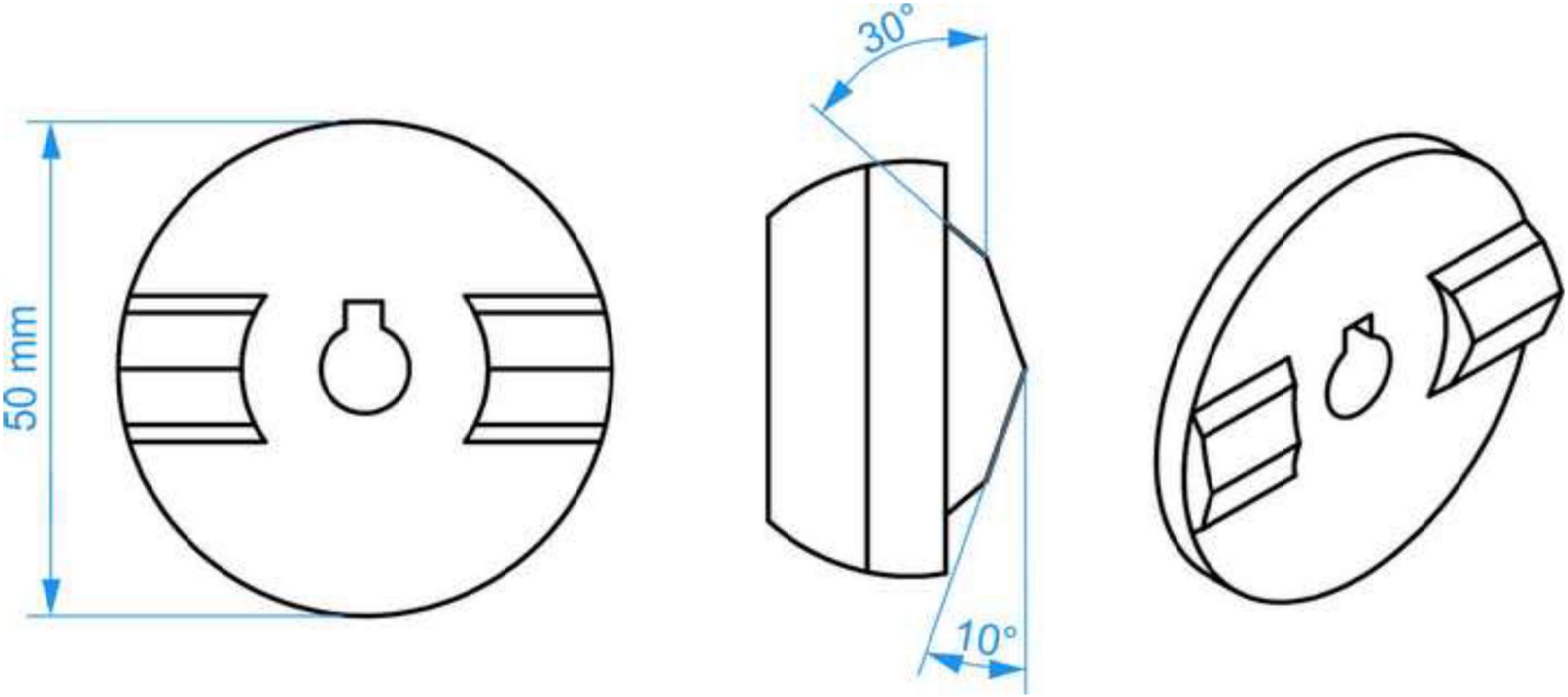

Figure 04

Click here to download high resolution image

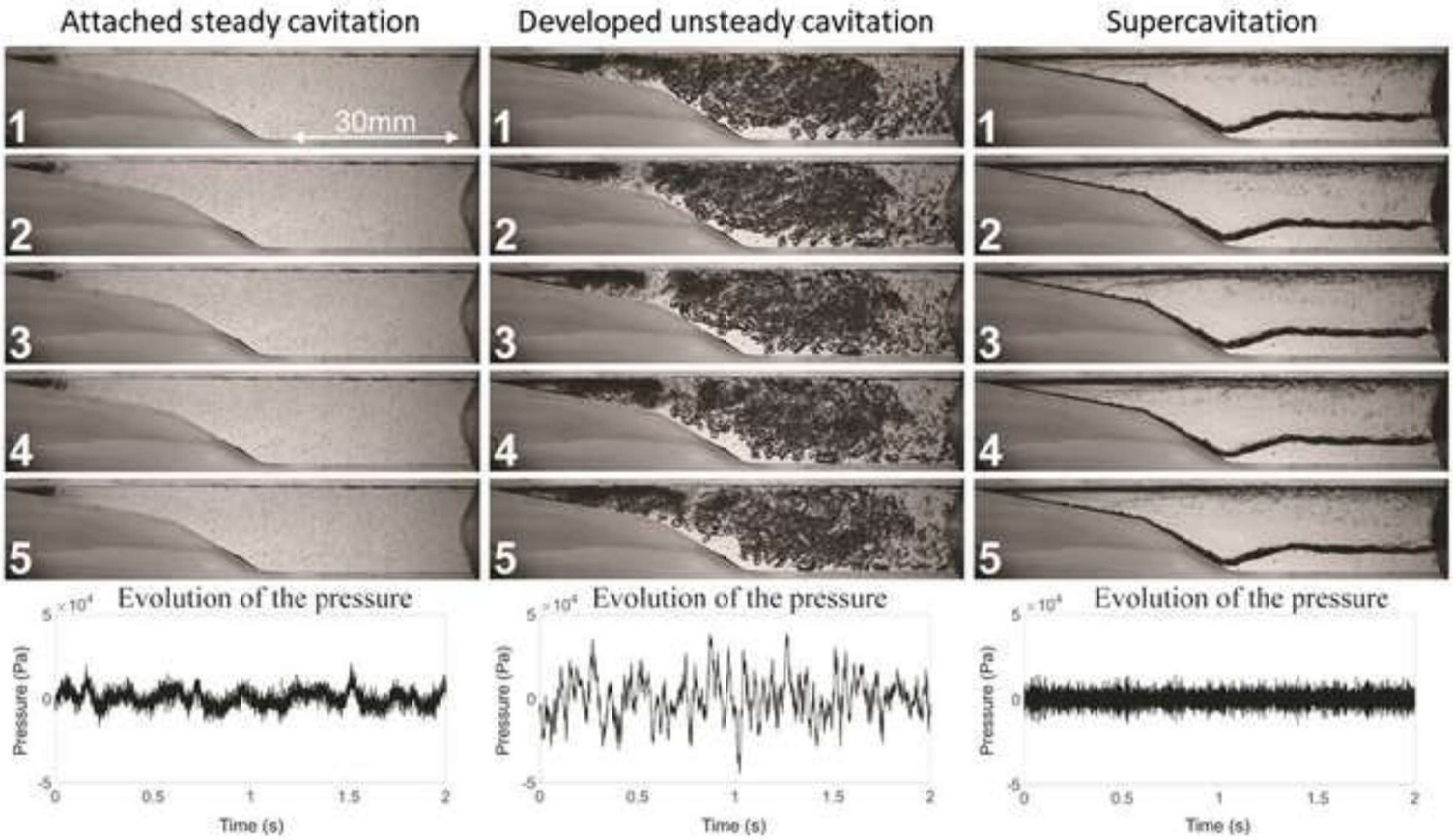

Figure 05
Click here to download high resolution image

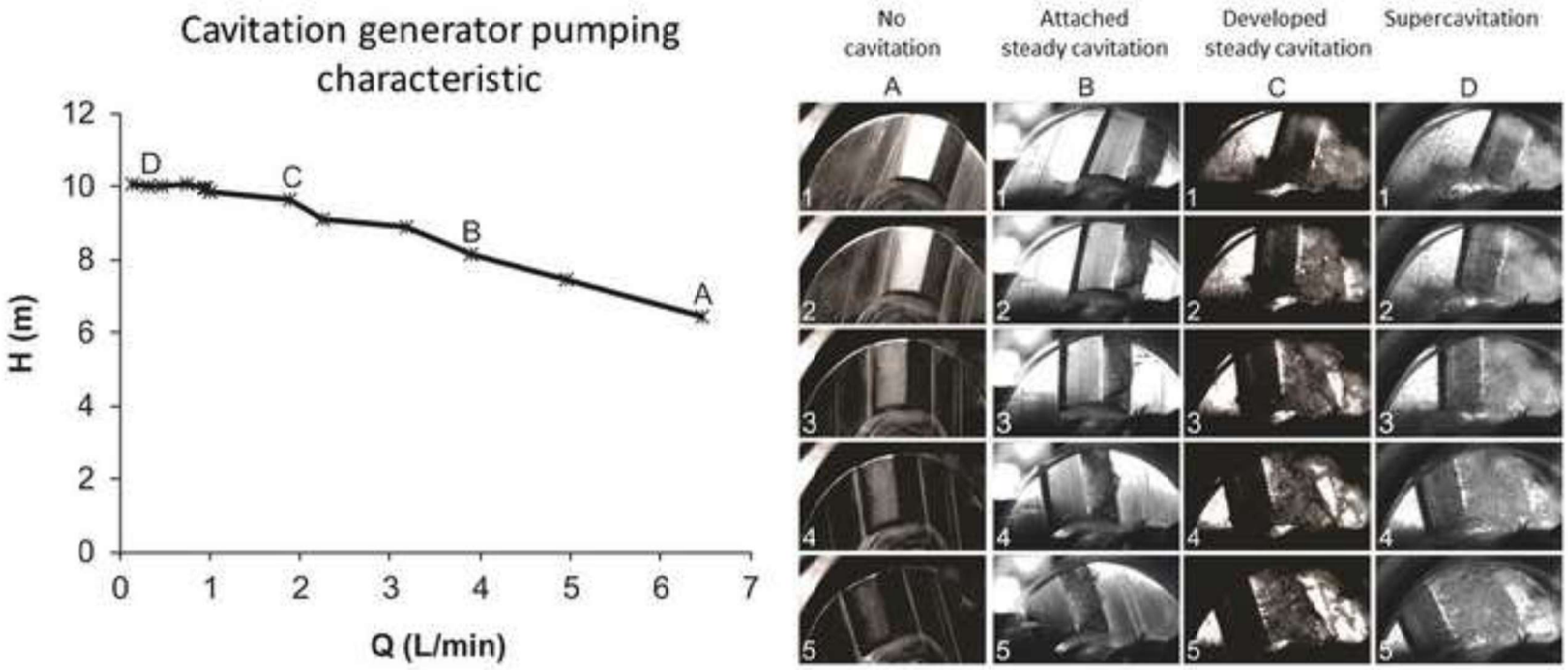

Figure 06
Click here to download high resolution image

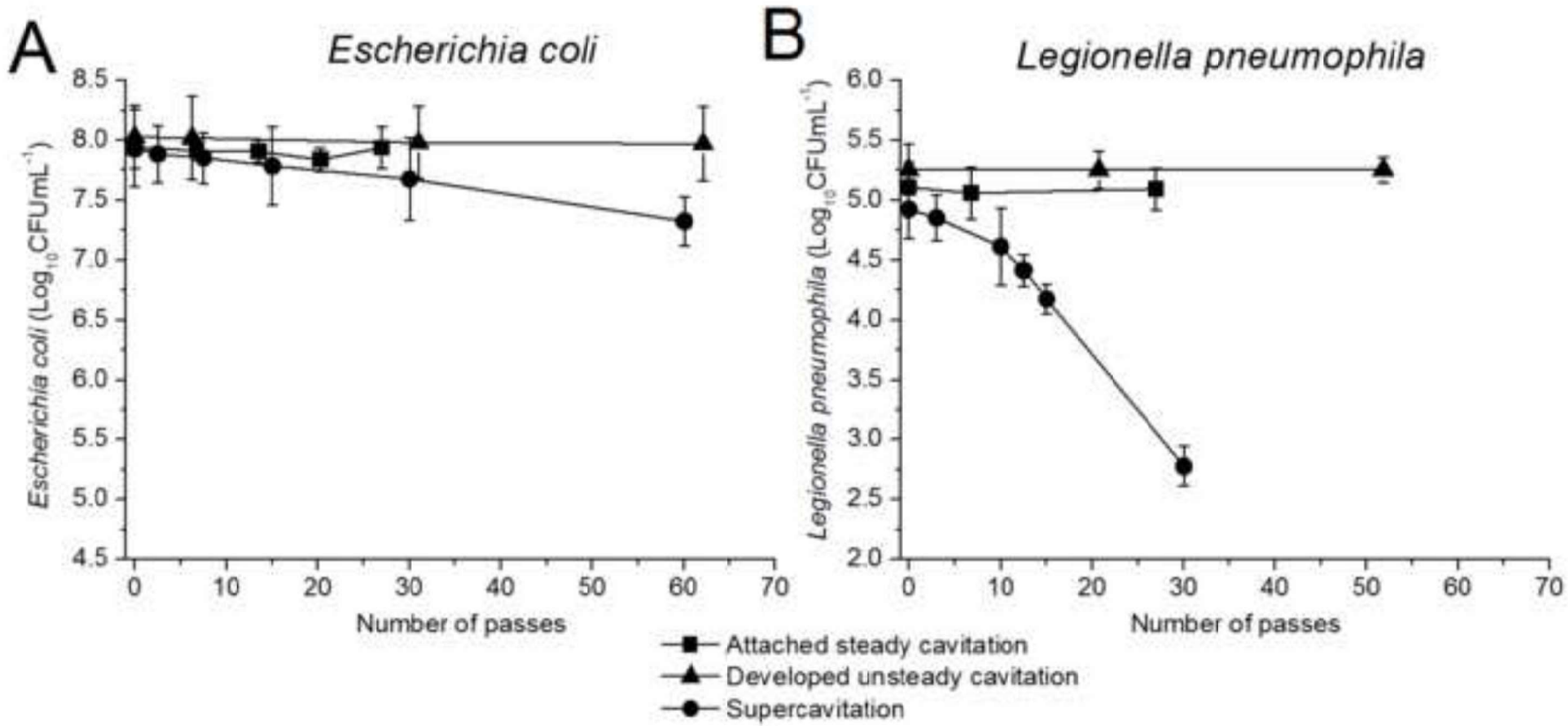

Figure 07
Click here to download high resolution image